

Aromaticities and reactivities based on energy partitioning

Yuansheng Jiang and Hongxing Zhang

Institute of Theoretical Chemistry, Jilin University, Changchun, P.R. China

Abstract - A scheme based on energy partitioning via moments is proposed to deal with aromaticities and reactivities of conjugated systems. The REPE is computed through the enumeration of cyclic fragments, thus either the finite or infinite systems can be treated with facility. Point-energy, edge-energy, and ring resonance energy have been introduced for rationalizing the site reactivity, bond lengths and local aromaticity. This approach is graphical in essence without consulting to the solution of secular equation, i.e., the energy sequence, MO(molecular orbital)'s and related quantities defined.

INTRODUCTION

In recent years, moments have attracted a considerable attention of theoreticians with particular interests in Hückel MO theory (ref. 1-5). The importance and advantage of utilizing moments rest upon their topological meaning in relationship to the connectivity of a molecule. Let us review their definition

$$u_1 = \sum_{j=1}^N x_j^1 = \text{Tr}(A^1) = \sum_{j=1}^N (A^1)_{jj} \quad (1)$$

where u_1 denotes the 1-th moment, A is the adjacency matrix with its elements being 1 when the row vertices and column vertices are connected by edges and zero otherwise, x_j ($j=1,2,\dots,N$) represents the j th-member of energy sequence.

Due to each term in the right-hand summation of Eq.(1) represents a self-adjoint walk of length 1 starting from vertex j , one can derive moment formulae in terms of molecular fragments one by one (ref.1,5). In the following, lower members are given with symbols and diagrams of fragments in Fig.1 for benzenoid hydrocarbons.

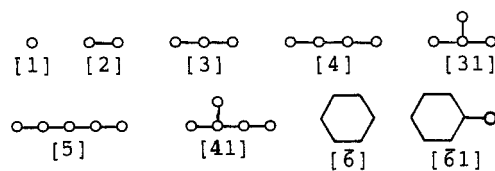


Fig.1. Elementary fragments in benzenoid hydrocarbons. [G] represents the fragment as well as its count.

$$\begin{aligned} u_0 &= [1] & u_2 &= 2[2] & u_4 &= 2[2]+4[3] \\ u_6 &= 2[2]+12[3]+6[4]+12[31]+12[\bar{6}] \\ u_8 &= 2[2]+28[3]+32[4]+72[31]+8[5]+16[41]+96[\bar{6}]+16[\bar{6}1] \end{aligned} \quad (2)$$

Moreover, one can classify molecular fragments into acyclic and cyclic species according to whether they involve at least one ring or not. Accordingly, u_1 can be partitioned into u_1' and u_1'' , the acyclic and cyclic components, fulfilling

$$u_1 = u_1' + u_1'' \quad (3)$$

In table 1, the fragment counts together with acyclic, cyclic and total values of moments ($1 \leq 8$) for naphthalene are tabulated for illustration.

Within the Hückel MO approximation, the total π -electron energy of the ground state of alternants and parts of non-alternants can be written as

$$E = 2 \sum_{i(\text{occ})} x_i = \sum_{i=1}^N |x_i| \quad (4)$$

Table 1. Moments (u_1' , u_1'' and u_1) and fragment counts of naphthalene with $l \leq 8$

	l=0	l=2	l=4	l=6	l=8
u_1'	10	22	78	322	1438
u_1''	0	0	0	24	256
u_1	10	22	78	346	1694
[1]=10	[2]=11	[3]=14	[4]=18	[31]=2	
[5]=22	[41]=8	[6]=2	[61]=4		

The absolute value $|x|$ can be expanded in terms of even powers of x (ref.1)

$$|x| = \alpha_0 + \alpha_2 x^2 + \alpha_4 x^4 + \dots + \alpha_{2L} x^{2L} + \dots \quad (5)$$

provided the point $x=0$ is excluded. In practice, Eq.(5) is truncated and coefficients $\alpha_0, \alpha_2, \dots, \alpha_{2L}$ can be determined numerically by least-squares fits in the interval, $-3.00 \leq x \leq 3.00$, or by expansion in terms of Chebyshev polynomials (ref.6). In Table 2, three numerical sets of α_{2L} for $L = 2, 4$ and 6 obtained by least square fits (ref.5) are tabulated.

Table 2. Numerical values of α_{2L} for $L = 2, 4$ and 6

L	α_0	α_2	α_4	α_6	α_8	α_{10}	α_{12}
2	0.3904	0.5262	-0.0283				
4	0.2393	0.9253	-0.2105	0.02733	-0.00130		
6	0.1783	1.2955	-0.6277	0.2042	-0.03565	0.00310	-0.000105

Accordingly, Eq.(4) can be transformed into

$$E = \alpha_0 u_0 + \alpha_2 u_2 + \dots + \alpha_{2L} u_{2L} \quad (6)$$

which is fundamental for dealing with aromaticities and reactivities.

AROMATICITY

The aromaticity of finite molecules has been investigated systematically on the idea expressed by Brelow and Dewar (ref.7-11). Among them, benzene is the most aromatic with largest REPE and has equal C-C bond lengths. On the other hand, graphite is an infinite hexagon lattice with equal C-C bond lengths approaching to benzene. Recently, Klein, Seitz and Schmalz (ref.12-14) studied a series of icosahedral carbon cages with graphite as a limit. They calculated REPE's by Hess-Schaad method (ref.9) which increase monotonously from C_{60} to C_{240} and approach to 0.053 for graphite. We intend to investigate the variation of aromaticity along with three imagined paths in detail when benzene is growing up to graphite. The general formula of REPE obtained for each homologous series exhibits a trend dependent on the dimensionality that the species is growing up. Let us discuss them below.

Spherical carbon cage C_N with I_h symmetry

Because moments can be divided into acyclic and cyclic components fulfilling Eq.(3), the total π -electron energy splits up too, i.e.,

$$E = E' + E'' \quad (7)$$

where E' , the acyclic energy is used to be the reference and the cyclic component E'' equals the resonance energy. Therefore,

$$REPE = \frac{E''}{N} = \frac{1}{N} \sum_{l=0}^L \alpha_{2l} u_{2l}'' = \frac{1}{N} \sum_{G''} \beta_{G''} [G''] \quad (8)$$

where $\beta_{G''}$ represents the energy contribution per fragment G'' which involves one ring at least. The numerical values of $\beta_{G''}$ have also been tabulated elsewhere (ref.5).

It can be proved that the only icosahedral cage structures that can be constructed form an infinite sequence with the number of vertices given by (ref. 12,14)

$$N = 20(h^2 + hk + k^2) \quad (0 \leq k \leq h) \quad (9)$$

with h and k integers. These cage structures are conveniently viewed by showing a single face of the master icosahedron on which each structure is based (ref. 15). Fig.2 illustrates such diagrams up to $N=540$.

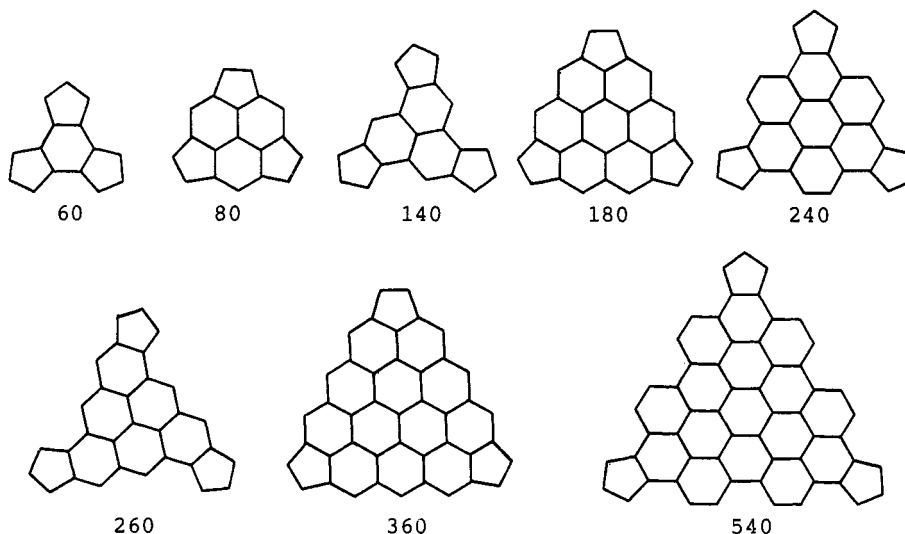


Fig.2. Repeat units for the icosahedral carbon cages

For these icosahedral cage structures, C_N 's, it is not difficult to carry out the cyclic components u_{21}'' one by one in terms of N . The formulae for $l=3, 4, 5$ and 6 are given as follows

$$\begin{aligned} u_6'' &= 6N - 120 \\ u_8'' &= 96N - 1920 \\ u_{10}'' &= 1110N - 22080 \\ u_{12}'' &= 11382N - 227160 + 3600\delta_{N,60} + 720\delta_{N,80} \end{aligned} \quad (10)$$

On substituting them into Eq.(8) and utilizing the coefficients for $L=6$ in table 1, we obtain the general formula for REPE for C_N

$$\text{REPE}(C_N) = 0.0489 - 0.657/N - (0.378\delta_{N,60} + 0.0756\delta_{N,80})/N \quad (11)$$

which gives a limit value of 0.0489 for graphite as $N \rightarrow \infty$. On the other hand, the ascending trend of $\text{REPE}(C_N)$ with respect to N is easily inspected from the differential below

$$d\text{REPE}(C_N)/dN = 0.657/N^2 > 0 \quad (N \neq 60, 80) \quad (12)$$

In Table 3, REPE's for closed shell carbon cages calculated according to Eq.(11) are tabulated up to $N=1980$, where values given by Klein, Seitz and Schmalz (KKS) are also listed for comparison.

Table 3. REPE's for C_N

C_N	Eq.(11)	KSS	C_N	Eq.(11)	KSS	C_N	Eq.(11)	KSS
C_{60}	0.032	0.031	C_{240}	0.046	0.047	C_{720}	0.048	
C_{80}^{6-}	0.040		C_{320}^{6-}	0.047		C_{960}^{6-}	0.048	
C_{140}^{6-}	0.044		C_{420}	0.047		C_{1980}	0.049	
C_{180}	0.045	0.045	C_{540}	0.048		Graphite	0.049	0.053

Polyacene and parallelogram-like hexagon lattice

Polyacene is a linearly fused benzenoid system with an arbitrary number of hexagons, n , and total vertices (the number of carbon atoms), $N=4n+2$. With the same procedure, one can derive the formulae for cyclic components u_{21}'' ($l=3-6$) at first, and substituting them into Eq.(8) with α_{21} 's of $L=6$, the formula of REPE is

$$\text{REPE}(n) = (0.0837n + 0.256 + 0.0766\delta_{n,1}) / (4n+2) \quad (13)$$

Its differential with respect to n is as follows

$$d\text{REPE}(n)/dn = -0.857/N^2 \quad (14)$$

This means that aromaticity of polyacene decreases monotonously with its chain lengths.

Let us consider the parallelogram-like species with n and m hexagons along the intersections of the parallelogram shown in Fig.3.

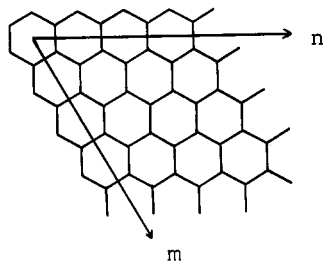


Fig.3. Two-dimensional benzenoid lattice

It represents a large number of benzenoid systems because n and m are arbitrary positive integers. For example, it reduces to polyacene when $m=1$. In the same way, the general formula of REPE for the parallelogram-like species displayed in Fig.3 can be also derived as follows

$$\text{REPE}(m,n) = [0.0489mn + 0.00222(m+n) + 0.0966] / (mn+m+n) \quad (m,n > 1) \quad (15)$$

It repeatedly gives the limit value, 0.0489, for graphite when m and n approach to infinite simultaneously. The partial differential of $\text{REPE}(m,n)$ with respect to n is equal to

$$\partial \text{REPE}(m,n) / \partial n = [0.0467m^2 - 0.0966(m+1)] / (mn+m+n)^2 \quad (16)$$

which induces the following conditions

$$\partial \text{REPE}(m,n) / \partial n \begin{cases} < 0 & \text{when } m < 3 \\ = 0 & \text{when } m = 2.8 \approx 3 \\ > 0 & \text{when } m > 3 \end{cases} \quad (17)$$

Eq.(17) means $m=3$ is a transition point below which ($m=1$ or 2) REPE decreases in proportion to the chain lengths of the polymer, on the contrary, the aromaticity of parallelogram-like benzenoid species increases with its length, n , if $m > 3$. These are better indicated in Fig.4.

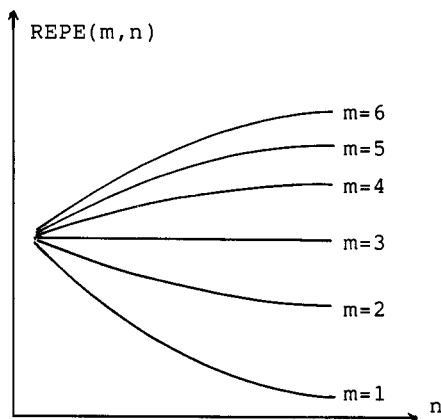


Fig.4. Qualitative tendency of $\text{REPE}(m,n)$ for parallelogram-like benzenoid species with definite m .

Kertesz and Hoffmann have examined the π -electron bands of the three members ($n=\infty$; $m=1,2,3$) of the lattice displayed in Fig.3 by extended Hückel calculations. They concluded that the energy gaps due to distortion sharply decreases

with the value of m in accordance with a power law for the energy gap openings (ref.16), i.e.,

$$E_g = c_m (\delta/B)^m \quad \text{with } |\delta/B| \ll 1 \quad (18)$$

This seems to agree with the behavior of REPE(m,n) that the partial differential $\partial \text{REPE}(m,n)/\partial n$ increases with the number of coupled polyacenic chains, m .

Benzenoid lattice with D_{6h} symmetry

For this species, let us enumerate the number of hexagons, n , from the center horizontally shown in Fig.5

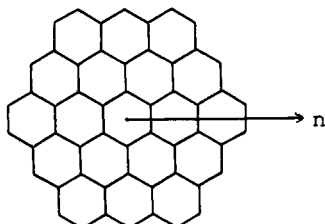


Fig.5. Benzenoid lattice with D_{6h} symmetry

Accordingly, we can derive the following formula

$$\text{REPE}(n) = 0.0489(1 - 1.5007/n + 2.0409/n^2) \quad (n > 1) \quad (19)$$

and find a transition point occurring at $n=3$, namely

$$d\text{REPE}(n)/dn = 0, \quad \text{if } n = 2.7 \approx 3 \quad (20)$$

The existence of transition points for aromaticity in the cases of lattices shown in Figs.3 & 5 comes from the competition between the di- and tri-valent vertices. As a result, one can think reasonably that in large benzenoid systems, the di-valent vertices play the role of anti-aromaticity, diminishing the value of REPE; on the other hand, tri-valent vertices behave aromatically, increasing the value of REPE. When the transition points are exceeded in the both cases, the tri-valent vertices increase sharply with chain lengths, leading to an ascending trend of REPE's.

SITE REACTIVITY AND BOND LENGTHS

As moment u_1 is defined in terms of self-adjoint walks, W_1^j ($j=1,2,\dots,N$), for each vertex (atom) which individualizes the vertex numerically, therefore, point-energy (ref.5) can be introduced for each carbon atom in accordance with

$$E = \sum_{j=1}^N E_j, \quad E_j = \sum_{l=0}^L \alpha_{2l} W_{2l}^j \quad (21)$$

where E_j is the point-energy of atom j , an well-behaved index in relation to site reactivity. As consequences, the following statements can be deduced.

(1). Site reactivity decreases as the vertex degree increases, namely, the mono-valent vertices are most active and tri-valent vertices are most inert.

(2). The site reactivities of atoms with equal valency are proportional to the valency of their adjacent atoms. This can be illustrated diagrammatically in Fig.6.

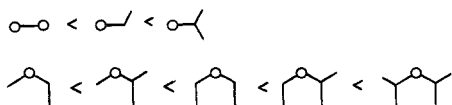


Fig.6. Sequences of site reactivities

Similarly, moments can be classified into edge components, W_1^e , and edge-energy (ref.5) can be defined accordingly,

$$E = N\alpha_0 + \sum_e E_e, \quad E_e = \sum_{l=1}^L \alpha_{2l} W_{2l}^e \quad (22)$$

where e is a current index for degrees (C-C). We have the following statements in addition.

(3). The bond length of an edge varies in proportion to its degree (Fig.7).

(4). For edges with equal degree, bond lengths vary in inverse proportion to degrees of their adjacent vertices (fig.7).

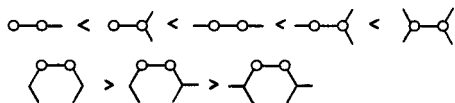


Fig.7. Ascending sequences of bond lengths in conjugated systems

LOCAL AROMATICITY

There have been considerable works (ref.17-19) on this topic. Here, we discuss local aromaticity by defining the resonance energy for a particular hexagon, h

$$(RE)_h = \sum_{r, G''} \beta_{G''} [G'']_r / n_r \quad (23)$$

where r runs through all rings enveloping the hexagon considered, n_r is the number of hexagons that the r th ring accommodates, and $[G'']_r$ enumerates cyclic fragment, G'' , covering the r th ring. An insight into the role of fragments can be inspected from Eq.(23). For example, there are four different types of hexagons in catafusenes (ref.18) shown in Fig.8. We can tabulate the counts of $[G'']_r$ of them in Table 4.

Table 4. $[G'']_r$ for various hexagons in catafusenes

$[G'']$	$\beta_{G''}$	P	L	K	T
$[\bar{6}1]$	-0.1535	2	4	4	6
$[\bar{6}11]$	0.02924	1	2	3	6
$[\bar{6}101]$	0.03176	0	2	2	6
$[\bar{6}1001]$	0.03176	0	2	1	3

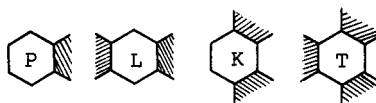


Fig.8. Four different types of hexagons in catafusenes

On comparing $[\bar{6}1]$, we have $(RE)_P > (RE)_L = (RE)_K > (RE)_T$. Furthermore, due to $\beta_{\bar{6}11} - \beta_{\bar{6}1001} < 0$, we have $(RE)_L > (RE)_K$. Therefore, we have a trend of local aromaticity for hexagons of catafusenes (ref.18): $P > L > K > T$.

REFERENCES

1. Y. Jiang, A. Tang and R. Hoffmann, Theoret. Chim. Acta, **66**, 183 (1984).
2. G.G. Hall, Theoret. Chim. Acta, **70**, 323 (1986) and references therein.
3. I. Gutman, Z. Markovic and S. Markovic, Chem. Phys. Lett., **134**, 139(1987).
4. S. Pick, Collection Czechoslovak Chem. Commum., **53**, 1607 (1988).
5. Y. Jiang and H. Zhang, Theoret. Chim. Acta, **75**, 279 (1989).
6. T.G. Schmalz, T. Ziviovic and D.J. Klein, Stud. Phys. Theoret. Chem., **54**, 173 (1988).
7. R. Breslow and E. Mohacsi, J. Am. Chem. Soc., **85**, 431 (1963).
8. M.J.S. Dewar and C. deLlano, J. Am. Chem. Soc., **91**, 789 (1969).
9. B.I. Hess, Jr. and L.T. Schaad, J. Am. Chem. Soc. **93**, 305 (1971).
10. J. Aihara, J. Am. Chem. Soc., **98**, 2750 (1976).
11. I. Gutman, M. Milun and N. Trinajstic, J. Am. Chem. Soc., **99**, 1692 (1977).
12. D.J. Klein, W.A. Seitz and T.G. Schmalz, Nature, **323**, 703 (1986).
13. T.G. Schmalz, W.A. Seitz, D.J. Klein and G.E. Hite, J. Am. Chem. Soc., **110**, 1113 (1988).
14. D.L.D. Caspar and A. King, Cold Spring Harbor Symp. on Quantitative Biology, **27**, 1 (1962).
15. P.W. Fowler, Chem. Phys. Lett., **131**, 444 (1986).
16. M. Kertesz and R. Hoffmann, Solid State Commun., **47**, 97 (1983).
17. O.E. Polansky and G. Derflinger, Int. J. Quantum Chem., **1**, 379 (1967).
18. M. Aida and H. Hosoya, Tetrahedron, **36**, 317 (1980).
19. K. Sakurai, K. Kitaura and K. Nishimoto, Theoret. Chim. Acta, **69**, 23 (1986).